AIAA JOURNAL
Vol. 34, No. 5, May 1996

Optimized Compact Finite Difference Schemes with Maximum Resolution

Jae Wook Kim* and Duck Joo Lee†
Korea Advanced Institute of Science and Technology, Taejon 305-701, Korea

Direct numerical simulations and computational aeroacoustics require an accurate finite difference scheme that has a high order of truncation and high-resolution characteristics in the evaluation of spatial derivatives. Compact finite difference schemes are optimized to obtain maximum resolution characteristics in space for various spatial truncation orders. An analytic method with a systematic procedure to achieve maximum resolution characteristics is devised for multidiagonal schemes, based on the idea of the minimization of dispersive (phase) errors in the wave number domain, and these are applied to the analytic optimization of multidiagonal compact schemes. Actual performances of the optimized compact schemes with a variety of truncation orders are compared by means of numerical simulations of simple wave convections, and in this way the most effective compact schemes are found for tridiagonal and pentadiagonal cases, respectively. From these comparisons, the usefulness of an optimized high-order tridiagonal compact scheme that is more efficient than a pentadiagonal scheme is discussed. For the optimized high-order spatial schemes, the feasibility of using classical high-order Runge–Kutta time advancing methods is investigated.

Nomenclature

a, b, c	= coefficients of compact discretization to be optimized
E	= integrated error of compact discretization in point of wave number range
e	= resolving efficiency
f	= objective function
f'	= spatial derivative of objective function
$\tilde{f}$	= Fourier transformed objective function
r	= optimization range factor
W	= weighting function for optimization of coefficients
α, β	= coefficients of compact discretization to be optimized
ε	= error tolerance
κ	= scaled true wave number
$\bar{\kappa}$	= scaled modified wave number
κ_f	= scaled critical wave number
ω	= true wave number
$\bar{\omega}$	= modified wave number
ω_f	= critical wave number

Introduction

RECENTLY, the need for a finite difference scheme that has a spatial and temporal high order of truncation has been increased for direct numerical simulations (DNS)[1–4] and computational aeroacoustics (CAA)[5–7] because the problems of DNS and CAA include high wave number (or high-frequency) and small-amplitude wave components. In addition to the high order of truncation, the high resolution of the scheme has been emphasized because it will determine the number of grid points per wavelength required to resolve the shortest wave component in the actual computation. The actual performance of a scheme with a time advancing method is dependent on both the truncation order and the degree of resolution.

Tam and Webb[7] increased the resolution of a spatial finite difference approximation by minimizing the integrated dispersive (phase) errors in the wave number domain and proposed the dispersion-relation-preserving (DRP) scheme. The coefficients of the central discretization are determined by the truncation order and the minimization of errors. The fourth-order spatial central scheme of an optimized seven-point stencil shows better resolution characteristics than the standard high-order unidiagonal central schemes.

The spatial resolution characteristics and the truncation order can be improved by using a multidiagonal compact discretization with a given stencil. Lele[8] showed the spectral-like resolution of the fourth-order pentadiagonal compact scheme for the evaluation of spatial derivatives. He found the coefficients of the compact discretization and achieved the spectral-like resolution by fitting the modified wave numbers to the corresponding true wave numbers. The fourth-order pentadiagonal scheme, which is a seven-point stencil for space, has been accurately used[8] with a fourth-order Runge–Kutta method for time advancing.

Consistent spatial–temporal finite difference schemes such as the leapfrog scheme and its variations[9] have been developed for the numerical simulation of waves or unsteady flows. Thomas and Roe[10] revised the leapfrog scheme to obtain a high order of truncation for spatial derivatives and time advancing and effectively used it as a high-order spatial–temporal scheme.

The main objective of this paper is an analytic optimization of the compact finite difference scheme and the optimization targets are the coefficients of its discretization. This paper shows that an analytic optimization produces the maximum spatial resolution characteristics of the compact finite difference approximation in the evaluation of the spatial finite derivatives. A Fourier analysis provides a way to optimize the compact schemes by quantifying the dispersive errors analytically. A method for the analytic optimization that was introduced by Tam and Webb[7] for the unidiagonal DRP scheme is to minimize the dispersive errors in the wave number domain, and this method is further developed in this paper in relation to the multidiagonal compact schemes with high order and high resolution. A weighting function is introduced in this procedure, which is a crucial step to achieve the analytic optimization for the multidiagonal compact schemes. The optimization ranges, in which the minimization of the dispersive errors is considered, are found to obtain the maximum resolution. With a systematic approach, the optimum coefficients of tridiagonal and pentadiagonal schemes are determined for various truncation orders, respectively.

Both the resolution and the truncation order of a compact scheme determine the overall error characteristics of its finite difference approximation in actual computations. And the actual error characteristics of the compact schemes are dependent on their multidiagonality (whether tridiagonal or pentadiagonal). The actual performances and accuracy of the optimized tridiagonal and

Received Nov. 26, 1994; revision received Dec. 15, 1995; accepted for publication Dec. 19, 1995.

*Graduate Student, Department of Aerospace Engineering, 373-1, Kusong-dong, Yusong-gu.

†Associate Professor, Department of Aerospace Engineering, 373-1, Kusong-dong, Yusong-gu. Member AIAA.

pentadiagonal compact schemes of various truncation orders can be compared only after numerical simulations with a time advancing method are followed to visualize their actual error characteristics. This paper presents the comparison between the optimized compact schemes with a variety of truncation orders for tridiagonal and pentadiagonal cases, respectively. The comparisons are made by means of the numerical simulations of simple wave convection, and the most effective tridiagonal and pentadiagonal schemes are found. Also, the usefulness of an optimized tridiagonal compact scheme, which is more efficient than a pentadiagonal one, is discussed in terms of the numerical comparisons.

Some numerical results with various orders of classical Runge–Kutta methods for temporal integration are presented to show the effects of spatial discretization on temporal integration.

Compact Discretization

The schemes presented here are generalizations of Padé scheme (see Refs. 8 and 11–13) based on a seven-point stencil as

$$\beta f'_{i-2} + \alpha f'_{i-1} + f'_i + \alpha f'_{i+1} + \beta f'_{i+2} = c\frac{f_{i+3} - f_{i-3}}{6\Delta x} + b\frac{f_{i+2} - f_{i-2}}{4\Delta x} + a\frac{f_{i+1} - f_{i-1}}{2\Delta x} \tag{1}$$

The finite difference equation that Tam and Webb[7] used for the dispersion-relation-preserving scheme is the unidiagonal ($\alpha = \beta = 0$) case of Eq. (1); that is, it is not a compact (multidiagonal) scheme. It is reasonable to expand such a unidiagonal finite difference equation to a multidiagonal one for the purpose of increasing the truncation order and resolution. The relations between the coefficients a, b, c, α, and β are derived by matching the Taylor series coefficients of various truncation orders. These relations are (see also Ref. 8)

Second order:

$$a + b + c = 1 + 2\alpha + 2\beta \tag{2}$$

Fourth order:

$$a + 2^2 b + 3^2 c = 2(3!/2!)(\alpha + 2^2\beta) \tag{3}$$

Sixth order:

$$a + 2^4 b + 3^4 c = 2(5!/4!)(\alpha + 2^4\beta) \tag{4}$$

Eighth order:

$$a + 2^6 b + 3^6 c = 2(7!/6!)(\alpha + 2^6\beta) \tag{5}$$

Tenth order:

$$a + 2^8 b + 3^8 c = 2(9!/8!)(\alpha + 2^8\beta) \tag{6}$$

Only the eighth-order tridiagonal ($\beta = 0$) scheme and the tenth-order pentadiagonal ($\beta \neq 0$) scheme have unique coefficients, and these are the highest order ones obtainable with this scheme. The other lower-order schemes must have free coefficients that are not determined until more constraints are imposed and these can be used to improve the resolution characteristics. The additional constraint that Lele[8] imposed is to fit the modified wave numbers to the corresponding true wave numbers for the purpose of increasing the resolution characteristics. Lele developed the fourth-order pentadiagonal scheme by using the constraints, and his results show an improved resolution characteristics in space. In this paper, other analytic and systematic constraints for determination of the free coefficients are considered. The nature of these constraints is the minimization of dispersive (phase) errors in the wave number domain; that is, the stencil wave number optimization introduced by Tam and Webb.[7]

Optimization of Coefficients

Fourier Analysis of Errors

The finite difference equation (1) is of a central difference, and thus it has no dissipative errors. In this section the differencing errors of Eq. (1) are analyzed in terms of the dispersive (phase) errors. A Fourier analysis provides an effective way to quantify the dispersive errors and resolution characteristics of a differencing approximation, and so this quantification will be used further to guide the analytic optimization of the differencing scheme. The finite difference equation (1) can be rewritten in the x direction as

$$\beta f'(x - 2\Delta x) + \alpha f'(x - \Delta x) + f'(x) + \alpha f'(x + \Delta x) + \beta f'(x + 2\Delta x) = c\frac{f(x + 3\Delta x) - f(x - 3\Delta x)}{6\Delta x} + b\frac{f(x + 2\Delta x) - f(x - 2\Delta x)}{4\Delta x} + a\frac{f(x + \Delta x) - f(x - \Delta x)}{2\Delta x} \tag{7}$$

The Fourier transform of the left and right sides of Eq. (7) is

$$i\omega[\beta \exp(-2i\omega\Delta x) + \alpha \exp(-i\omega\Delta x) + 1 + \alpha \exp(i\omega\Delta x) + \beta \exp(2i\omega\Delta x)]\tilde{f} = \{(c/6\Delta x)[\exp(3i\omega\Delta x) - \exp(-3i\omega\Delta x)] + (b/4\Delta x)[\exp(2i\omega\Delta x) - \exp(-2i\omega\Delta x)] + (a/2\Delta x)[\exp(i\omega\Delta x) - \exp(-i\omega\Delta x)]\}\tilde{f} \tag{8}$$

From this equation, the (scaled) modified wave number is derived (see also Ref. 8) as

$$\bar{\omega}\Delta x \equiv \frac{a \sin(\omega\Delta x) + (b/2)\sin(2\omega\Delta x) + (c/3)\sin(3\omega\Delta x)}{1 + 2\alpha\cos(\omega\Delta x) + 2\beta\cos(2\omega\Delta x)} \tag{9}$$

The modified wave number, defined in Eq. (9), is used for the analysis of finite difference errors. It is a periodic function of $\omega\Delta x$ (the scaled true wave number) with a period of 2π. To ensure that the Fourier transform of the finite difference scheme is a good approximation of the partial derivative, the modified wave number should coincide with the corresponding true wave number ($\bar{\omega} = \omega$) over as wide a range of wave numbers (i.e., $0 \leq \omega\Delta x < \pi$) as possible. As the modified wave number deviates from the true wave number, the finite difference errors (dispersive errors) are produced.

Minimization of Errors

An integrated error (weighted deviation) is defined in this paper (see also Ref. 7) as

$$E \equiv \int_0^{r\pi} (\omega\Delta x - \bar{\omega}\Delta x)^2 W(\omega\Delta x)\, \mathrm{d}(\omega\Delta x) \tag{10}$$

where $W(\omega\Delta x)$ is a weighting function, and r is a factor to determine the optimization range ($0 < r < 1$) under consideration. The integrated error defined in Eq. (10) is different from that of Tam and Webb[7] in that it contains the weighting function and the range factor r (see Refs. 7 and 14). The weighting function in Eq. (10) makes the equation analytically integrable and also allows the integrand to be weighted in the high wave number range (near π) where most dispersive errors exist. The integrated error for this scheme is expressed as

$$E = \int_0^{r\pi} \left(\kappa - \frac{(c/3)\sin(3\kappa) + (b/2)\sin(2\kappa) + a\sin(\kappa)}{1 + 2\alpha\cos(\kappa) + 2\beta\cos(2\kappa)}\right)^2 \times W(\kappa)\, \mathrm{d}\kappa \tag{11}$$

where $\kappa = \omega\Delta x$. The integrated error in Eq. (11) is a function of the coefficients a, b, c, α, and β. It is necessary to find the optimum values of the coefficients that minimize the integrated error. The

conditions that make E a local minimum value are proposed by Tam and Webb[7] as follows:

$$\frac{\partial E}{\partial a} = 0 \tag{12}$$

$$\frac{\partial E}{\partial b} = 0 \tag{13}$$

$$\frac{\partial E}{\partial c} = 0 \tag{14}$$

$$\frac{\partial E}{\partial \beta} = 0 \tag{15}$$

$$\frac{\partial E}{\partial \alpha} = 0 \tag{16}$$

Equations (2–6) and (12–16) provide a system of linear algebraic equations by which the optimum coefficients can be determined. The optimization procedure to determine the coefficients a, b, c, α, and β for maximum resolution characteristics is as follows:

1) Tridiagonal ($\beta = 0$):
   Second order: Solve Eqs. (2), (13), (14), and (16).
   Fourth order: Solve Eqs. (2), (3), (14), and (16).
   Sixth order: Solve Eqs. (2), (3), (4), and (16).
2) Pentadiagonal ($\beta \neq 0$):
   Second order: Solve Eqs. (2), (13–15), and (16).
   Fourth order: Solve Eqs. (2), (3), (14), (15), and (16).
   Sixth order: Solve Eqs. (2–4), (15), and (16).
   Eighth order: Solve Eqs. (2–5) and (16).

Weighting Function

The weighting function proposed in this paper, $W(\kappa)$, can be chosen to make Eq. (11) integrable as follows:

$$W(\kappa) = [1 + 2\alpha \cos(\kappa) + 2\beta \cos(2\kappa)]^2 \tag{17}$$

Note that the unidiagonal central scheme used in Ref. 7 does not need such a weighting function, because $\alpha = \beta = 0$, which presents no problem in integrating E analytically. The weighting function presented in Eq. (17) can be used to evaluate the integrated error in Eq. (11) analytically; however, it may not weight the integrated error sufficiently in the high wave number range where a lot of dispersive errors occur. Thus it is necessary to revise the weighting function in Eq. (17) so as to weight the integrated error more than enough in the high wave number range close to π, by multiplying an exponential term as follows:

$$W(\kappa) = \{[1 + 2\alpha \cos(\kappa) + 2\beta \cos(2\kappa)]e^{\kappa}\}^2 \tag{18}$$

By weighting the integrated error more in the high wave number range than in the low wave number range, as a result, the dispersive errors in the high wave number range can be more reduced through the optimization procedure.

Optimization Ranges

In the case of the optimization range factor $r = 1$ (full range optimization), the resolution characteristics of the optimized compact schemes obtained by the optimization procedure and the weighting function of Eq. (17) are compared with those of other standard finite difference schemes in Fig. 1. It is evident that the optimized schemes have a tendency to stay closer to the exact differentiation over a wider range of wave numbers than the other nonoptimized standard schemes. However, there is considerable overshoot (the largest deviation from the exact differentiation in the optimization range) in each optimized scheme as shown in Fig. 1. The scaled modified wave number defined in Eq. (9) falls to a value of zero when the scaled true wave number is π. Thus most dispersive errors exist in the range $0.9\pi \leq \omega\Delta x \leq \pi$, and it is preferable that this wave number range should be omitted in the optimization. Minimizing the errors in the range near π is meaningless and inefficient, and so the effects of optimization shown in Fig. 1 are not satisfactory.

In the case of reducing the optimization range factor to $r = 0.9$, the resolution characteristics of the optimized compact schemes obtained by the optimization procedure and the weighting function of Eq. (18) are compared with those of other standard finite difference schemes in Fig. 2. In this case there are remarkable improvements in the resolution as expected; that is, the optimized schemes tend to stick to the exact differentiation over a wider range of wave numbers than those of the previous case. This is because the wave number range near π, where a lot of errors that are definitely uncontrollable exist, is not considered any more in the optimization procedure. The lower the order of truncation, the better the resolution achieved, because greater numbers of constraints minimizing the integrated error are applied. Thus it seems a lower-order scheme may obtain better resolution characteristics than a higher-order scheme.

For $r = 0.9$, each scheme still has noticeable overshoot, and this should be reduced to below 0.5% of the corresponding true wave

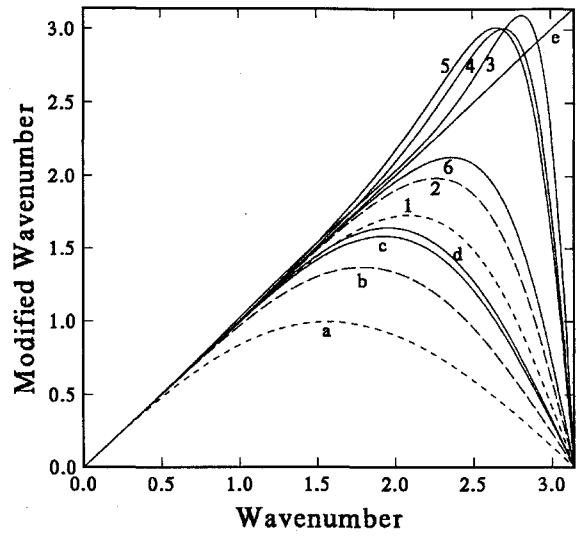

a) Comparison of the tridiagonal schemes with others

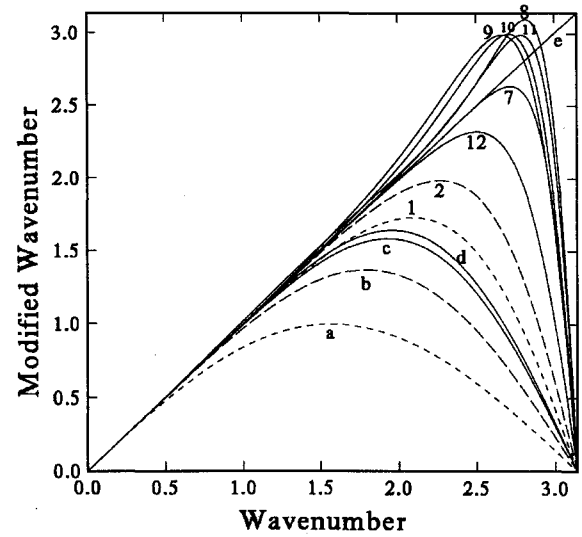

b) Comparison of the pentadiagonal schemes with others

Fig. 1 Plots of the modified wave number vs true wave number (r = 1.0): a—second-order central differences, b—fourth-order central differences, c—sixth-order central differences, d—Tam's DRP scheme, e—exact differentiation, 1—standard Padé scheme, 2—sixth-order tridiagonal scheme (c = 0), 3—optimized second-order tridiagonal scheme, 4—optimized fourth-order tridiagonal scheme, 5—optimized sixth-order tridiagonal scheme, 6—eighth-order tridiagonal scheme, 7—Lele's fourth-order spectral-like pentadiagonal scheme, 8—optimized second-order pentadiagonal scheme, 9—optimized fourth-order pentadiagonal scheme, 10—optimized sixth-order pentadiagonal scheme, 11—optimized eighth-order pentadiagonal scheme, and 12—tenth-order pentadiagonal scheme; ——, 7-point stencil; – – –, 5-point stencil; and - - - -, 3-point stencil.

Table 1 Optimized coefficients for maximum resolution characteristics

Tridiagonal	a	b	c	α	β
Second order	1.545790417	0.434249728	−0.078236437	0.450901855	0
Fourth order	1.551941906	0.361328195	−0.042907397	0.435181352	0
Sixth order	1.568098212	0.271657107	−0.022576781	0.408589269	0

Table 2 Optimized coefficients for maximum resolution characteristics

Pentadiagonal	a	b	c	α	β
Second order	1.265667929	1.079904285	0.053798648	0.596631925	0.103053504
Fourth order	1.280440844	1.049309076	0.044465832	0.589595521	0.097512355
Sixth order	1.323482375	0.944394243	0.027596356	0.566458285	0.081278202
Eighth order	1.373189728	0.814447053	0.016707870	0.537265947	0.064906379

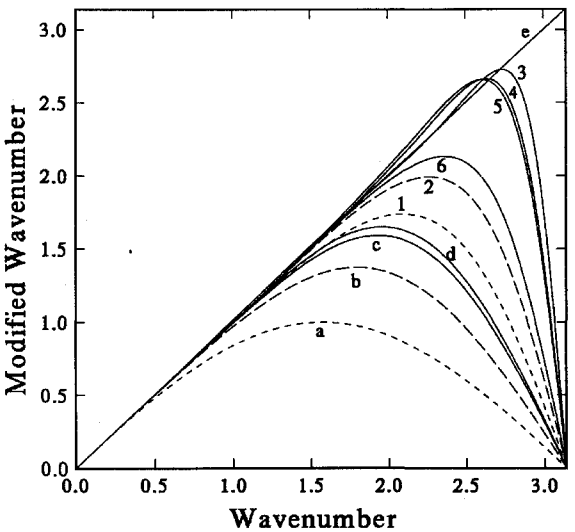

a) Comparison of the tridiagonal schemes with others

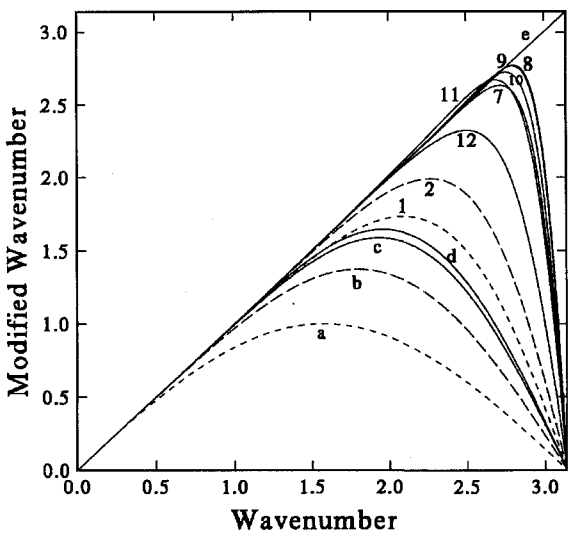

b) Comparison of the pentadiagonal schemes with others

Fig. 2 Plots of the modified wave number vs true wave number (r = 0.9): a—second-order central differences, b—fourth-order central differences, c—sixth-order central differences, d—Tam's DRP scheme, e—exact differentiation, 1—standard Padé scheme, 2—sixth-order tridiagonal scheme (c = 0), 3—optimized second-order tridiagonal scheme, 4—optimized fourth-order tridiagonal scheme, 5—optimized sixth-order tridiagonal scheme, 6—eighth-order tridiagonal scheme, 7—Lele's fourth-order spectral-like pentadiagonal scheme, 8—optimized second-order pentadiagonal scheme, 9—optimized fourth-order pentadiagonal scheme, 10—optimized sixth-order pentadiagonal scheme, 11—optimized eighth-order pentadiagonal scheme, and 12—tenth-order pentadiagonal scheme; ——, 7-point stencil; – – –, 5-point stencil; and - - - -, 3-point stencil.

Table 3 Resolving efficiency $e(\varepsilon)$ of various schemes shown in Fig. 3

	ε		
Schemes	0.1	0.01	0.005
a) Second-order central difference	0.250	0.078	0.055
b) Fourth-order central difference	0.443	0.239	0.200
c) Sixth-order central difference	0.543	0.350	0.309
d) Tam's DRP scheme	0.622	0.450	0.414
1) Standard Padé scheme	0.593	0.355	0.301
2) Sixth-order tridiagonal (c = 0)	0.732	0.548	0.500
3) Optimized second-order tridiagonal	0.875	0.813	0.803
4) Optimized fourth-order tridiagonal	0.853	0.780	0.769
5) Optimized sixth-order tridiagonal	0.813	0.715	0.700
6) Eighth-order tridiagonal	0.754	0.583	0.538
7) Lele's spectral-like scheme	0.900	0.836	0.820
8) Optimized second-order pentadiagonal	0.928	0.890	0.885
9) Optimized fourth-order pentadiagonal	0.923	0.882	0.876
10) Optimized sixth-order pentadiagonal	0.902	0.851	0.843
11) Optimized eighth-order pentadiagonal	0.871	0.800	0.788
12) Tenth-order pentadiagonal	0.817	0.681	0.643

numbers for tolerable accuracy. The optimization range factors of each scheme need to be readjusted to obtain maximum resolution characteristics as follows:

1) Tridiagonal ($\beta = 0$):
   Second order: $r = 0.820$
   Fourth order: $r = 0.790$
   Sixth order: $r = 0.715$
2) Pentadiagonal ($\beta \neq 0$):
   Second order: $r = 0.90$
   Fourth order: $r = 0.890$
   Sixth order: $r = 0.865$
   Eighth order: $r = 0.815$

The coefficients obtained by using each of the preceding optimization range factors and the weighting function of Eq. (18) for each scheme are presented in Tables 1 and 2 for the tridiagonal and the pentadiagonal schemes, respectively. The maximum resolution characteristics of the optimized compact schemes with the coefficients in Tables 1 and 2 obtained by the optimization procedure and the weighting function of Eq. (18) are compared with those of other standard finite difference schemes in Fig. 3. Each scheme has a small overshoot that is less than 0.5% of the corresponding true wave number and thus tolerable, and each sticks close to the exact differentiation over a progressively large wave number range compared with other standard schemes.

Resolving Efficiency

The range of wave numbers $[0, \kappa_f]$, over which the modified wave number approximates the exact differentiation ($\bar{\omega} = \omega$) within a specified error tolerance, defines a set of well-resolved waves. The value κ_f ($= \omega_f \Delta x$), which gives the shortest well-resolved wave, depends on the specified error tolerance. It is reasonable to keep this error tolerance fixed when different finite difference schemes are compared. In the following, the error tolerance is defined (see also Ref. 8) as

$$\frac{|\bar{\kappa}(\kappa) - \kappa|}{\kappa} \leq \varepsilon \tag{19}$$

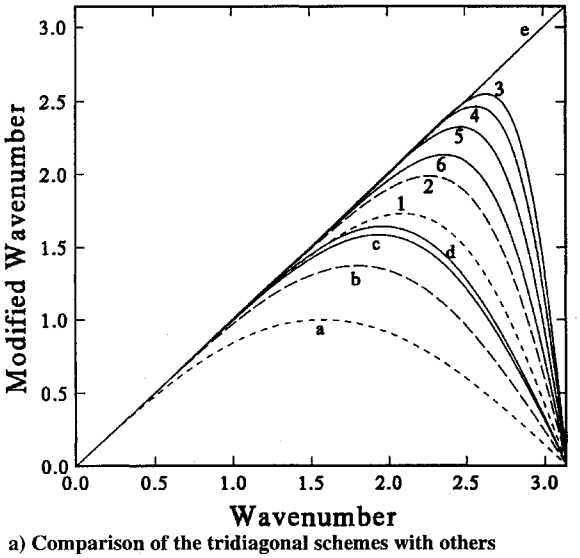

a) Comparison of the tridiagonal schemes with others

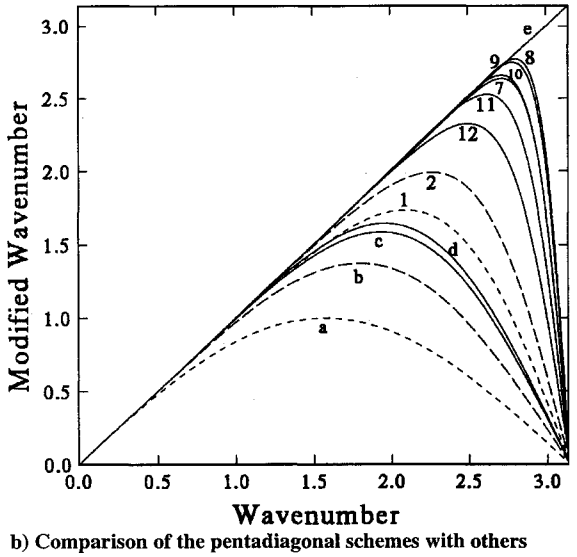

b) Comparison of the pentadiagonal schemes with others

Fig. 3 Plots of the modified wave number vs true wave number with the coefficients optimized for maximum resolution characteristics: a—second-order central differences, b—fourth-order central differences, c—sixth-order central differences, d—Tam's DRP scheme, e—exact differentiation, 1—standard Padé scheme, 2—sixth-order tridiagonal scheme (c = 0), 3—optimized second-order tridiagonal scheme, 4—optimized fourth-order tridiagonal scheme, 5—optimized sixth-order tridiagonal scheme, 6—eighth-order tridiagonal scheme, 7—Lele's fourth-order spectral-like pentadiagonal scheme, 8—optimized second-order pentadiagonal scheme, 9—optimized fourth-order pentadiagonal scheme, 10—optimized sixth-order pentadiagonal scheme, 11—optimized eighth-order pentadiagonal scheme, and 12—tenth-order pentadiagonal scheme; ——, 7-point stencil; – – –, 5-point stencil; and - - - -, 3-point stencil.

where $\bar{\kappa} = \bar{\omega}\Delta x$. And the fraction $e(\varepsilon)$, defined next, may be regarded as a measure of the resolving efficiency of a scheme:

$$e(\varepsilon) \equiv (\omega_f \Delta x)/\pi = \kappa_f/\pi \tag{20}$$

The resolving efficiencies of the optimized compact schemes with the coefficients in Tables 1 and 2 are presented in Table 3 and are compared with other standard schemes.

Applications to Simple Waves

This section illustrates an application of the optimized compact schemes to some initial value problems of a wave equation,

$$\frac{\partial f}{\partial t} + \frac{\partial f}{\partial x} = 0, \qquad t > 0 \tag{21}$$

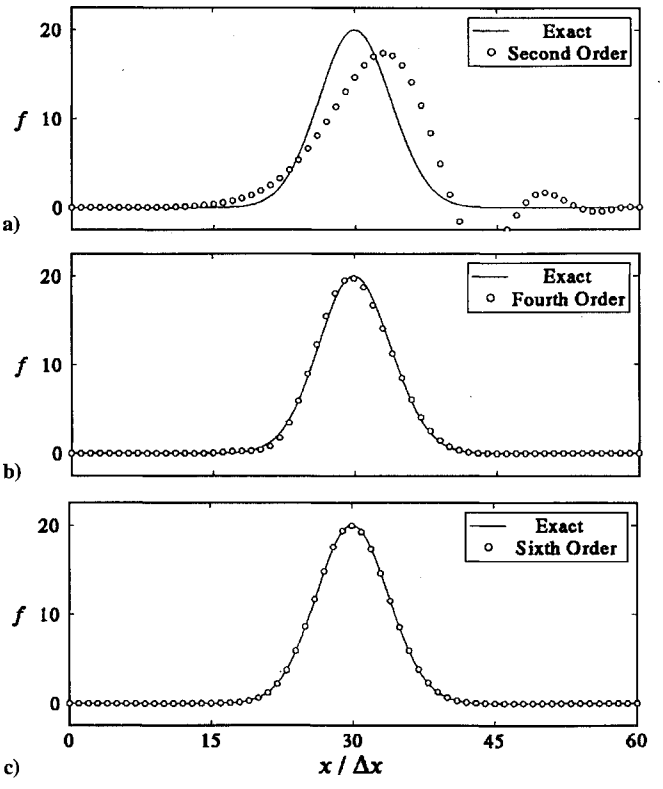

Fig. 4 Application of the tridiagonal schemes to bell-shaped wave [Courant-Friedrichs-Lewy (CFL) number = 0.5 and t = 5000Δt]: a) optimized second-order tridiagonal scheme, b) optimized fourth-order tridiagonal scheme, and c) optimized sixth-order tridiagonal scheme.

Convection of simple waves is numerically simulated by the optimized compact schemes of various truncation orders in the evaluation of spatial derivatives. The classical fourth-order Runge–Kutta method is used for temporal integration. The results with a given number of grid points for each initial wave shape are presented in Figs. 4–7.

In Fig. 3, it is noted that an optimized lower-order compact scheme has more resolution in the wave number domain than an optimized higher order one, but it is expected that the lower-order scheme may produce more truncation errors (actual errors in space) than the higher order one. Both the resolution in the wave number domain and the truncation order in space of a compact scheme determine the overall error characteristics of its finite difference approximation in actual computations. Also, the actual error characteristics of the compact schemes are dependent on their multidiagonality (whether tridiagonal or pentadiagonal). Thus, it is not easy to see the actual performance of the optimized tridiagonal and pentadiagonal compact schemes until some numerical simulations are followed to visualize their actual error characteristics and compare their actual accuracy as shown in Figs. 4–7.

Notice that the optimized sixth-order tridiagonal and the optimized fourth-order pentadiagonal schemes provide solutions that have fewer dispersive errors and thus retain the initial shape of a wave longer than the other compact schemes. In other words, these have the best combinations of the resolution characteristics and the order of truncation, and so these seem to be the most effective compact schemes. The optimized sixth-order tridiagonal scheme is found to be efficient and economic because its actual performance is comparable to the optimized pentadiagonal schemes, although it needs only a tridiagonal matrix solver that is easy and fast for computation.

Determination of the number of grid points per wavelength needed in the actual simulation must be made to correctly capture the convection of the shortest wavelength component. The determinations can be made by using the critical scaled wave numbers of the optimized compact schemes. As presented in Table 3, the critical scaled wave numbers that can be resolved by

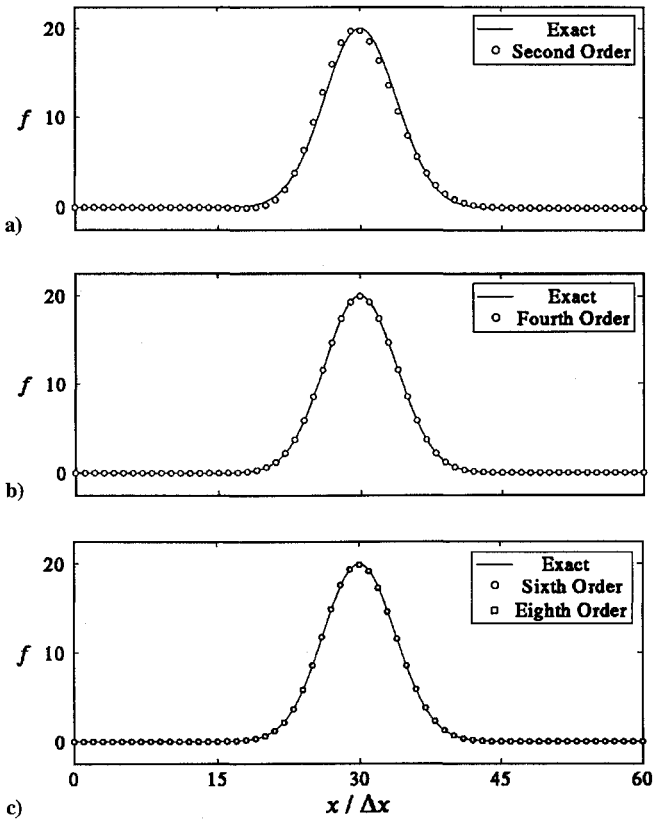

Fig. 5 Application of the pentadiagonal schemes to bell-shaped wave (CFL = 0.5 and $t = 5000\Delta t$): a) optimized second-order pentadiagonal scheme, b) optimized fourth-order pentadiagonal scheme, and c) optimized sixth- and eighth-order pentadiagonal schemes.

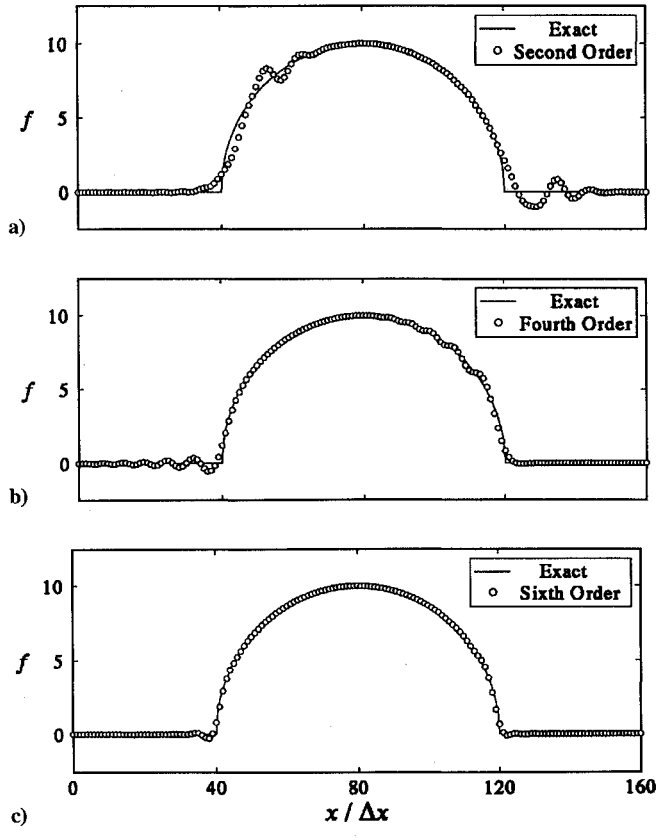

Fig. 6 Application of the tridiagonal schemes to semicircular wave (CFL = 0.5 and $t = 5000\Delta t$): a) optimized second-order tridiagonal scheme, b) optimized fourth-order tridiagonal scheme, and c) optimized sixth-order tridiagonal scheme.

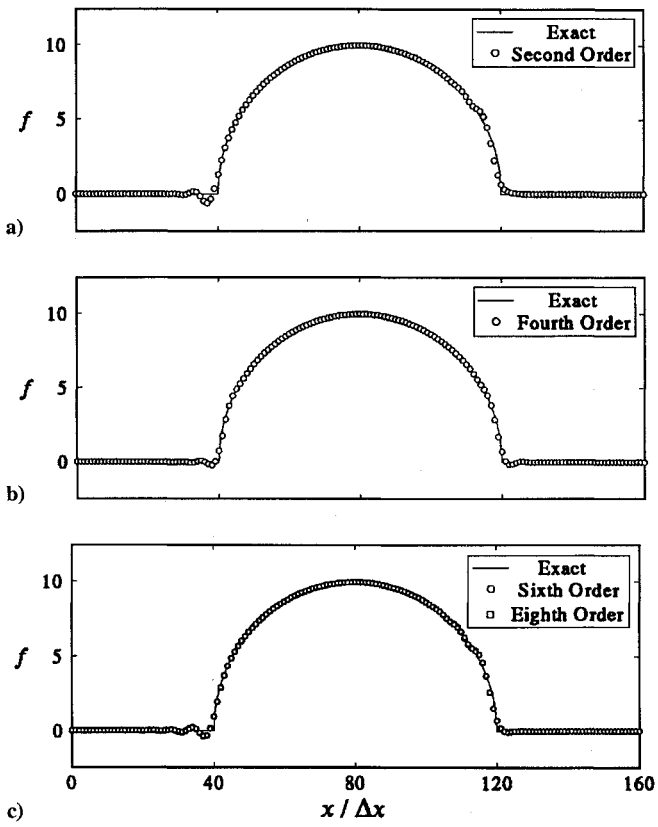

Fig. 7 Application of the pentadiagonal schemes to semicircular wave (CFL = 0.5 and $t = 5000\Delta t$): a) optimized second-order pentadiagonal scheme, b) optimized fourth-order pentadiagonal scheme, and c) optimized sixth- and eighth-order pentadiagonal scheme.

the optimized sixth-order tridiagonal scheme and the optimized fourth-order pentadiagonal scheme are 0.700 π and 0.876π, respectively. With these critical scaled wave numbers specified, the critical number of grid points can be determined by fast Fourier transform (FFT).

The differencing schemes described here provide improved resolution characteristics of small length scales. And the schemes have a pure central difference form; that is, they have no built-in artificial dissipation. They are, however, restricted to problems with smooth solutions. If they are to be applicable to problems with highly discontinuous solutions, they must be developed to be able to detect discontinuities and eliminate noisy oscillations. Since uniformly nonoscillatory (UNO) schemes with an artificial compression method[15] (ACM) have good resolution characteristics near the discontinuities, they can be used to capture shocks and contact surfaces. Therefore, the hybrids of optimized compact schemes and UNO schemes with an ACM can be applied to problems with highly discontinuous solutions.

In more complex applications such as nonlinear acoustic problems, numerical viscosity terms will be needed. For example, Tam's recent implementations of the dispersion-relation-preserving scheme use an adaptive filter[5] that can remove the spurious oscillations confined to a narrow range of high wave numbers. Addition of these filters to the optimized compact schemes will give a solution possibly with much less oscillation near discontinuities. But if the optimized compact schemes are to be used with an adaptive filter, it seems that the target range of wave numbers to be damped out by the adaptive filter should be concentrated on those of a higher range near π.

For a high-order spatial scheme, a high-order Runge–Kutta time advancing method seems to be necessary not to lose the overall truncation order, but it is found that it is not always required to keep this correspondence between the spatial and temporal schemes. Comparison between the classical Runge–Kutta methods of various orders is presented in Fig. 8. This comparison can be made by application of these methods to Eq. (21) with the optimized fourth-order

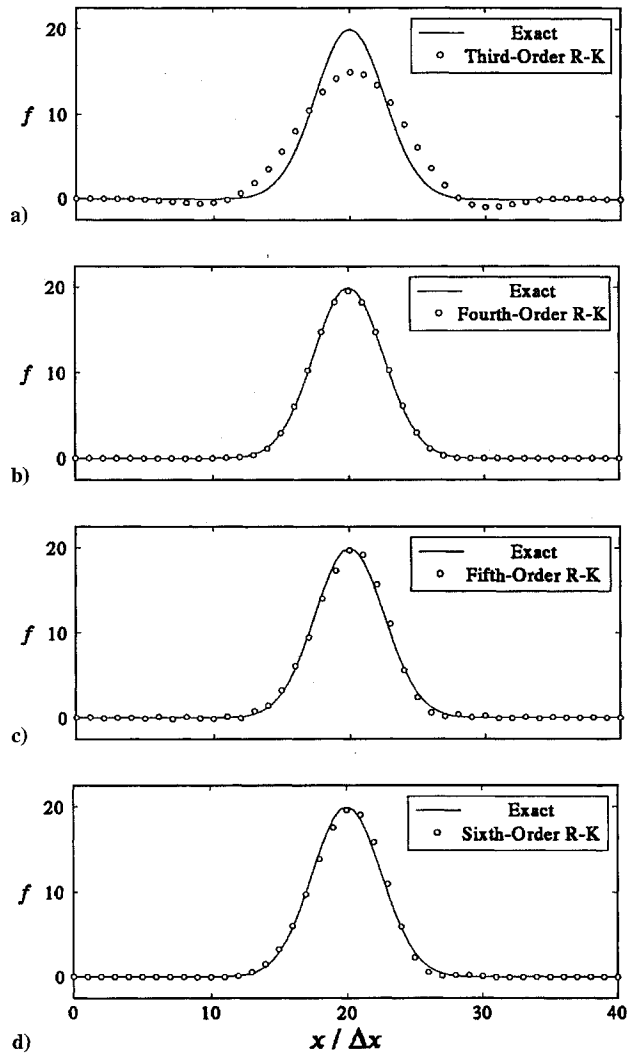

Fig. 8 Comparison between the classical Runge–Kutta methods of various orders (CFL = 0.5 and $t = 5000\Delta t$): a) classical third-order Runge–Kutta method, b) classical fourth-order Runge–Kutta method, c) classical fifth-order Runge–Kutta method, and d) classical sixth-order Runge–Kutta method.

pentadiagonal scheme in space. In Fig. 8, one can see that the classical fourth-order Runge–Kutta method provides a solution that has little dispersive error, and the higher orders (the fifth and sixth) are no better than the fourth order. Similar results emerge for the cases with sixth- or eighth-order spatial schemes. A classical higher-order Runge–Kutta method requires more stages and computation time but provides no better solutions than the fourth order. It is recommended to investigate the possible use of high-order spatial schemes with the classical fourth-order Runge–Kutta method rather than those of higher order.

Conclusions

In this paper, high-order compact finite difference schemes are optimized analytically to achieve maximum resolution characteristics. The analytic optimization method and procedure suggested here for the multidiagonal compact schemes are also useful for the other spatial or temporal finite difference schemes to obtain high-resolution characteristics. The sixth-order tridiagonal and fourth-order pentadiagonal schemes are successfully optimized to be the most effective and accurate compact schemes for actual computations. The usefulness of the optimized sixth-order tridiagonal compact scheme that is very efficient compared with the pentadiagonal schemes is discussed in this paper. It is pointed out that the overall error characteristics of the optimized compact schemes in actual computation are dependent on the truncation order, the resolution, and their multidiagonality (whether tridiagonal or pentadiagonal). The classical fourth-order Runge–Kutta time advancing shows better results than the higher order ones for the optimized high-order compact schemes in space.

References

[1]Clarksean, R., "Direct Numerical Simulation of a Plane Jet Using the Spectral-Compact Finite Difference Technique," AIAA Paper 91-0197, Sept. 1990.

[2]Lele, S. K., "Direct Numerical Simulation of Compressible Free Shear Flows," AIAA Paper 89-0374, Jan. 1989.

[3]Colonius, T., Lele, S. K., and Moin, P., "Scattering of Sound Waves by a Compressible Vortex," AIAA Paper 91-0494, Jan. 1991.

[4]Mitchell, B. E., Lele, S. K., and Moin, P., "Direct Computation of the Sound from a Compressible Co-Rotating Vortex Pair," AIAA Paper 92-0374, Jan. 1992.

[5]Tam, C. K. W., Webb, J. C., and Dong, Z., "A Study of the Short Wave Components in Computational Acoustics," *Journal of Computational Acoustics*, Vol. 1, No. 1, 1993, pp. 1–30.

[6]Chen, C. L., and Liu, Y., "Analysis of Numerical Approaches for Acoustic Equations," AIAA Paper 93-4324, Oct. 1993.

[7]Tam, C. K. W., and Webb, J. C., "Dispersion-Relation-Preserving Schemes for Computational Aeroacoustics," *Journal of Computational Physics*, Vol. 107, No. 2, 1993, pp. 262–281.

[8]Lele, S. K., "Compact Finite Difference Schemes with Spectral-Like Resolution," *Journal of Computational Physics*, Vol. 103, No. 1, 1992, pp. 16–42.

[9]Iserles, A., "Generalized Leapfrog Methods," *IMA Journal of Numerical Analysis*, Vol. 6, No. 3, 1986, pp. 381–392.

[10]Thomas, J. P., and Roe, P. L., "Development of Non-Dissipative Numerical Schemes for Computational Aeroacoustics," AIAA Paper 93-3382, July 1993.

[11]Lomax, H., "Recent Progress in Numerical Techniques for Flow Simulation," *AIAA Journal*, Vol. 14, No. 4, 1976, pp. 512–518.

[12]Collatz, L., *The Numerical Treatment of Differential Equations*, Springer–Verlag, New York, 1966, p. 538.

[13]Kopal, Z., *Numerical Analysis*, Wiley, New York, 1961, p. 552.

[14]Kim, J. W., and Lee, D. J., "Optimized Compact Finite Difference Schemes for Solving Wave Equations," *Proceedings of the First Joint CEAS/AIAA Aeroacoustics Conference* (16th AIAA Aeroacoustic Conf.), Vol. 1, AIAA, Washington, DC, 1995, pp. 65–74.

[15]Ko, D. K., and Lee, D. J., "Third Order UNO Schemes with an ACM for Linear Waves and Euler Equations," *Proceedings of the 5th International Symposium on Computational Fluid Dynamics*, Vol. 2, Japan Society of Computational Fluid Dynamics, Tokyo Noko Univ., Tokyo, Japan, 1993, pp. 59–64.